

ZK-IMG: Attested Images via Zero-Knowledge Proofs to Fight Disinformation

Daniel Kang
UIUC

Tatsunori Hashimoto
Stanford

Ion Stoica
Berkeley

Yi Sun
University of Chicago

Abstract

Over the past few years, AI methods of generating images have been increasing in capabilities, with recent breakthroughs enabling high-resolution, photorealistic “deepfakes” (artificially generated images with the purpose of misinformation or harm). The rise of deepfakes has potential for social disruption. Recent work has proposed using ZK-SNARKs (zero-knowledge succinct non-interactive argument of knowledge) and attested cameras to verify that images were taken by a camera. ZK-SNARKs allow verification of image transformations non-interactively (i.e., post-hoc) with *only* standard cryptographic hardness assumptions. Unfortunately, this work does not preserve input privacy, is impractically slow (working only on 128×128 images), and/or requires custom cryptographic arguments.

To address these issues, we present ZK-IMG, a library for attesting to image transformations while hiding the pre-transformed image. ZK-IMG allows application developers to specify high level image transformations. Then, ZK-IMG will transparently compile these specifications to ZK-SNARKs. To hide the input or output images, ZK-IMG will compute the hash of the images inside the ZK-SNARK. We further propose methods of chaining image transformations securely and privately, which allows for arbitrarily many transformations. By combining these optimizations, ZK-IMG is the first system to be able to transform HD images on commodity hardware, securely and privately.

1 Introduction

In recent years, *deepfakes* have been proliferating. Deepfakes are “videos and images that have been digitally manipulated to depict people saying and doing things that never happened” [26]. One common use of deepfakes is to fool viewers for the purpose of misinformation, typically on social media [26]. They have also been used to fool companies into sending money to hackers [21] and fake personas to seed misinformation for business scams [35]. Their ability to

fool and prevalence has been driven by artificial intelligence methods [27, 29].

The rise of deepfakes raises a critical question: how can we verify the authenticity of visual media in the face of malicious adversaries? Furthermore, many applications have additional desiderata. First, the image from the camera should be able to be *transformed* by a series of permissible transforms from the source image. For example, an image should be able to be cropped or selectively blurred to exclude sensitive information. Second, the visual media should be verifiable *non-interactively*, or after the image has been taken and transformed. Non-interactivity is particularly important for social media as social media providers and consumers are not present at the time of image generation. Third, arbitrary third parties should be able to verify the transformed image.

One method to attest to transformed images is to combine attested cameras (which sign images immediately on being taken) with cryptographic techniques to verify the transformations. In particular, ZK-SNARKs (zero-knowledge succinct non-interactive argument of knowledge) allow arbitrary computations to be verified without revealing any information about the inputs or intermediate steps of the computation. Furthermore, Zk-SNARKs are non-interactive and produce certificates that any third party can verify.

Unfortunately, prior work for ZK-SNARKs for image edits are impractical for several reasons [8, 20, 25]. First, *they require revealing the original or intermediate images to verify the transformations* [8, 25]. If the original image could be released, then there is no need for private image transformations as the verifier can replay the transformations. Although these protocols could be modified to address this shortcoming, we show that doing so can add up to $20\times$ overheads. Second, they operate on only images that are impractically small (128×128 or smaller) [8, 25]. Third, they require custom arguments for specific image transformations [20, 25]. For example, some prior work can only perform image crops [20].

As a first step towards verification of visual media, we present ZK-IMG, the first system to attest the validity of *arbitrary and arbitrarily many* image transforms on HD (720p)

images on commodity hardware. ZK-IMG takes as input a camera-attested image and a high-level specification of the transformations to apply. It then produces a ZK-SNARK proof of the transformations and the output image. ZK-IMG can attest transformations of HD images on commodity hardware, which is two orders of magnitude larger than prior work.

To produce ZK-SNARK proofs, ZK-IMG leverages recent *general-purpose* ZK-SNARK proving systems, specifically `halo2` [39]. We demonstrate how to efficiently implement a wide range of image transforms in `halo2`, including “physical” transformations (crops, rotations, flips, translations, resizes), colorspace conversions (RGB to YCbCr and YCbCr to RGB), filters (sharpen, blur), and other standard operations (white balance, contrast adjustment). We implement these efficiently in ZK-IMG by fusing operations and packing computations efficiently in the ZK-SNARK construction.

In addition to implementing individual image operations, we also provide an end-to-end method of chaining together *arbitrarily many* image transformations without revealing the intermediate outputs. To do so, ZK-IMG will pack as many transformations into a single proof as possible. If not all transformations fit in a single proof, ZK-IMG will split them across proofs. To avoid revealing information in this process, ZK-IMG hashes the inputs and outputs and reveals only the hashes as part of the proofs. Only the final output is revealed. By combining these optimizations, ZK-IMG is able to verify arbitrarily many image transforms on HD images on commodity hardware.

We evaluate ZK-IMG on a range of image transformations. We show that ZK-IMG can produce proofs for HD image transformations that can be verified in as little as *5.6 milliseconds* on commodity hardware. Furthermore, ZK-IMG can prove end-to-end image transformations on commodity hardware, costing as little as \$0.48.

In the remainder of the paper, we provide background on deepfakes in Section 2, use cases in Section 3, and ZK-SNARK in Section 4. We describe ZK-IMG’s architecture in Section 6 and its detailed implementation in Sections 7 and 8. We evaluate ZK-IMG in Section 9. Finally, we discuss related work in Section 10 and conclude in Section 11.

2 Background

In recent years, purposeful spread of fake information and impersonations have increased in prevalence and capabilities. There are many malicious uses for such capabilities including spreading misinformation on social media [1, 37], fooling businesses to wire money to hackers [34], and others. Furthermore, these actors can range from state actors to “lone-wolf” hackers [12, 36].

Deepfakes. One way of spreading this misinformation is through the use of deepfakes. Deepfakes are “a specific kind of synthetic media where a person in an image or video is



Figure 1: An example of a deepfake [33]. As shown, another person’s likeness can be replaced in the image realistically. Although this example is innocuous, deepfakes have been used for malicious purposes, including theft and the spread of misinformation.

swapped with another person’s likeness” [31]. We show an example in Figure 1 [33].

In recent years, deepfakes have been increasing in their realism. This is driven in large part due to advances in machine learning (ML) methods, in particular generative ML methods. For example, models such as Stable Diffusion [29] and others can generate photorealistic images and edit existing images with high fidelity.

As such, deepfakes have already been used to spread misinformation (e.g., to fool soldiers into surrendering by faking heads of states) [36] and steal money (e.g., by impersonating a CEO’s voice) [34]. Finding solutions to deepfakes is an important and challenging problem.

Attested cameras. One proposal to help address the problem of deepfakes are *attested cameras*. Attested cameras contain hardware elements that can digitally sign images *immediately on capture*. Attested cameras further contain hardware elements to ensure that the camera is tamper-proof and the private key cannot be extracted without being destroyed.

Given these capabilities, attested cameras can attest that an image was taken by a particular camera. In this work, we assume the existence of secure (i.e., tamper-proof) attested cameras.

Using attested cameras. Given the existence of attested cameras, several organizations (e.g., C2PA) and prior work has proposed using these cameras to combat deepfakes. In particular, consumers of digital media can verify that a camera took a particular image without any assumptions of trust (beyond standard cryptographic assumptions).

However, raw images are rarely released in practice. In practice, nearly all released images are edited [24]. These edits are used to remove sensitive information, increase the legibility of the image, and for improved visual quality.

The image edits create a security challenge: the edits must be attested if the original attested image is not released. Image

edits can be attested by software systems. However, this creates additional surface area for attackers: if a malicious actor can access the editing software private key, they can sign arbitrary images. As many users who aim to attest to image edits are non-experts, this can be unacceptable in high-stakes scenarios. For example, state actors can compel citizens to give up their private keys, but camera manufacturers can discard private keys after manufacturing.

In the remainder of this work, we describe several use cases for verified image transformations and how to attest to image edits in a trustless manner.

3 Use Cases

Verified image transformations have uses in a range of settings, which have different application requirements. We describe several example use cases and their requirements below.

Verified images with redaction and editing. One important use case is to verify an edited image where the original image is hidden. Verifiers wish to ensure that the images are from an attested camera and image producers wish to redact and edit the image. For example, a news organization may wish to redact bystander faces or confidential information. In the setting of social media, verifiers cannot trust the image producers due to malicious adversaries. In this setting, the original image cannot be revealed. Thus, prior work that reveals the original image cannot be used in this setting.

Attesting to hidden images. Another important use case is to attest to an edited image where the edited image is hidden until some later point in time. To understand why this is desired, consider the famous “situation room” photo of former President Obama in the white house during Operation Neptune Spear [4]. Neither the original image nor the edited image can be revealed at the time the image was taken. Furthermore, the camera cannot be connected to the internet for security purposes, which makes trusted third parties (TPPs) for timestamps infeasible.

Some applications may also desire to attest to a hidden image so that the hidden, edited image can be used in downstream applications. For example, these hidden images can subsequently be used as inputs to machine learning models for biometric identification, where the user wishes to hide the image.

In this setting, the image producer can post a hash and signature of the original image, a ZK-SNARK of the edit *and a hash of the edited image*. Namely, the output image is not revealed, only the hash. By publishing the hash and proof (e.g., on a storage server or blockchain), the image producer can prove that the image was taken before the output image is revealed.

4 ZK-SNARKS and Halo2

4.1 Overview

In this work, we are interested in verifying function execution. Namely, let $y = f(x; w)$, where x is the *public input*, w is the *private input*, and y is the output. In our setting, the public input x is hash of the pre-transformed image, the private input w is the pre-transformed image itself, and y is either the hash of the output image or the output image itself.

ZK-SNARKs allow a *prover* to produce a proof π that can convince a *verifier* of the function execution, where the verifier only has access to π , y , and x [3]. We defer a full description of ZK-SNARKs and their properties to [3], but highlight several of its properties.

For the purposes of image transformation attestation, ZK-SNARKs are *non-interactive* and *zero-knowledge*. Namely, they do not require communication between the prover and verifier beyond π , so the proof can be verified at any point in time. They also reveal no information about w beyond what is already revealed in x and y . As such, they satisfy the criteria we outlined above.

ZK-SNARKs are also *succinct* (have short and easy to verify proofs), *complete* (correct proofs will verify successfully), and *knowledge sound* (computationally bounded provers cannot generate proofs of invalid executions).

ZK-SNARK proof generation typically involves two steps. The first step, arithmetization, turns the computation into a system of polynomial equations over a large finite field that hold if and only if the computation evaluates correctly. The second step uses a cryptographic proof system (i.e., a *backend*) to generate the proof from the polynomial equations.

In this work, we use the Halo2 proving system [39], implemented in the `halo2` software library. Halo2 uses the Plonkish arithmetization, which contains several features that are useful for numeric computations beyond previous proving systems (e.g., Groth16). We now describe the Plonkish arithmetization and performance considerations with Halo2.

4.2 Plonkish Arithmetization and Halo2

We now describe the Plonkish arithmetization. We begin by describing its logical operations from an application developer perspective, an example of how to implement a simple circuit, and conclude with performance considerations.

Plonkish arithmetization (logical operations). We first describe the *logical* operations allowed in the Plonkish arithmetization from an application developer perspective. In this section, we use `numpy` indexing notation where possible.

In the Plonkish arithmetization, the variables of the polynomials take values in a large prime field and are arranged in a rectangular grid. We denote this grid as $c[i][j]$, where i is the row index and j is the column index.

The first logical operation allowed in the Plonkish arithmetization is a *copy* operation, which is equivalently an equality operation. The equality operation enforces that two chosen cells in the grid have equal values, namely that $c[i][j] == c[i'][j']$ for chosen indexes i, j, i' , and j' .

The second logical operation allowed in the Plonkish arithmetization is a *lookup* operation. The lookup operation requires a set of lookup columns, $c[:, j_1', j_2', \dots, j_n']$. Given these columns, the lookup operation enforces that the columns in a given row must be in the lookup columns. Namely, for a row i and a set of columns j_1, j_2, \dots, j_n , the lookup argument enforces

$$c[i][j_1, \dots, j_n] = c[i'][j_1', \dots, j_n']$$

for some row index i' in the grid.

The third logical operation allowed in the Plonkish arithmetization is a *custom gate* operation. The custom gate operation enforces a polynomial constraint on some configuration of rows and columns in a fixed pattern. Namely, let $(a_1, b_1), (a_2, b_2), \dots, (a_n, b_n)$ be offset indexes. Then, for some polynomial f taking n variables, the custom gate enabled on row i enforces that

$$f(c[i + a_1][b_1], \dots, c[i + a_n][b_n]) = 0$$

In many cases, a_i is zero, so the custom gate applies only over a single row. The application developer may select which rows the custom gate applies to.

Example. To demonstrate how each operation is used, we provide a toy example. Consider the setting where a prover wishes to prove that they know values a, b , and c such that $a + b = 5, a + c = 7$ and $a \in \{0, \dots, 3\}$. The prover wishes to keep a, b , and c hidden.

There are a number of ways to construct an arithmetic circuit satisfying the properties. As we discuss below, different constructions have performance implications. We choose a particular construction for the purpose of this example.

We first lay out the grid as follows

	0	1	2	3
0	a	b	5	0
1	a	c	7	1
2	-	-	-	2
3	-	-	-	3

where the cells with dashes indicate that they can take arbitrary values. In this construction, we reveal column 2 as public inputs.

We then apply one equality operation, one lookups, and one custom gate:

1. We use the equality operator to enforce that $c[0][0] == c[1][0]$, which constrains the first two cells in the first column to be equal to some value, which we denote a .
2. We use the lookup to enforce that $c[0][0]$ takes a value in column 3. This enforces that $a = c[0][0] \in \{0, \dots, 3\}$.

3. We use a custom gate that enforces $c[i][0] + c[i][1] - c[i][2] = 0$ (i.e., the row offsets are all 0). We apply this custom gate on rows 0 and 1. Since $c[0][2]$ and $c[1][2]$ are revealed, this enforces that $a + b = 5$ (in row 0) and that $a + b = 7$ (in row 1).

As mentioned, there are a number of ways to construct arithmetic circuits to satisfy the constraints. As an example, instead of using a single custom gate with a public column, we could have instead used two custom gates that constrain $c[i][0] + c[i][1] - 5 = 0$ and $c[i][0] + c[i][1] - 7 = 0$, and removed column 2.

Additionally, we could have removed column 3 and instead used a custom gate to enforce that $a \in \{0, \dots, 3\}$. The custom gate would be $c[i][0] * (c[i][0] - 1) * (c[i][0] - 2) * (c[i][0] - 3) = 0$. By using this custom gate, we can also omit rows 2 and 3.

As we discuss below, choices of arithmetization can have dramatic effects on performance.

Halo2. `halo2` is a library that implements ZK-SNARK proving via the Plonkish arithmetization [39]. Its “frontend” accepts specifications of Plonkish arithmetic circuits. Given a circuit specification, `halo2` compiles the circuit to a ZK-SNARK via a cryptographic “backend.” We use a KZG-based backend, which has small proof sizes (relative to other ZK-SNARK backends) [19].

5 Arithmetization Performance Considerations

We now describe the intuition behind the implementation of the Plonkish logical operations and its performance implications.

Although an accurate cost model for Plonkish circuits is difficult to construct, computing relative costs is straightforward. Namely, reducing the number of rows, columns, permutation arguments, and lookup tables will almost always reduce the computational costs. Furthermore, for two circuits with the same number of permutation arguments, number of lookup tables, and *total* grid size, the circuit with the smaller number of rows will typically be cheaper. Finally, for the circuits we consider, the maximum polynomial degree is fixed, so it is irrelevant for relative cost considerations.

To understand why, we describe several salient properties of Plonkish circuits. We focus on the grid size, lookup tables, and custom gates.

First, the computational burden of both proving and verification scales with the number of rows and columns in the grid (although not necessarily linearly in the total number of cells). As a result, minimizing grid size is imperative.

Second, the number of rows in a valid grid *must be a power of two*. This constraint is enforced as the proving system operates over subgroups of the large finite field, which are of size 2^k for some k . This constraint is critical. For example,

consider a circuit with $2^k + 1$ rows with useful values (i.e., values that are constrained). Then, the circuit must be size 2^{k+1} . Thus, the number of rows is critical.

Third, in order to implement a lookup, the proving system internally adds an extra column, two equality constraints (which is internally a “permutation argument”), and a low degree custom gate. These additions are in addition to the lookup column. Furthermore, to enforce the zero knowledge property of the lookup table, the proving system adds t extra rows to the lookup table (where t depends on the security parameter of the proving system). This is particularly salient for image transformations since a lookup table of size 2^{24} actually requires $2^{24} + t$ rows, which forces the grid to have at least 2^{25} rows.

Fourth, the proving system internally adds an extra column for every custom gate as well. In particular, denote the extra column to be s_i . The proving system replaces the polynomial f with $s \cdot f$. Then, in order to “select” a row, the proving system sets $s_i = 1$, so that $s_i \cdot f = f$. In order to “deselect” a row, the proving system sets $s_i = 0$ so that $s_i \cdot f = 0$.

The final setup, proving, and verification times are complex functions of the number of rows, number of columns, number of permutation arguments, number of lookup tables, and the highest degree of the custom gate. Modeling the computational burden for a given circuit is difficult as a result.

6 ZK-IMG Architecture

ZK-IMG is a library which takes as input an attested image and a high-level specification of image transformations. It outputs the transformed image one or more ZK-SNARK proofs attesting to the validity of the image transformations. ZK-IMG further allows applications developers to specify new image transformations.

One critical requirement is the ability to specify *multiple* image transformations. Unfortunately, there is no work that allows multiple image transformations to be securely *and* privately applied in sequence. We describe how to accomplish this via ZK-IMG in Section 8.

At a high level, ZK-IMG operates by determining the maximum number of image transformations it can place in a single ZK-SNARK proof, given the hardware resources available. It then splits the chain of transformations based on these constraints and produces a ZK-SNARK proof for each subset of transformations. As we describe below, the verification key contains information about the transformation. This verification key is specific to the transformation but the generation can be amortized for many common transformations (resizing to standard sizes, color space conversions, blurring filters, etc.).

To do so, ZK-IMG contains two components: a high-level optimizer and cost-modeler for placing transformations, a transpiler for arithmetizing image transformations, and an

execution engine to produce the individual ZK-SNARKs. We describe the components in more detail below.

We now describe ZK-IMG’s security model and its limitations.

Security model. ZK-IMG assumes the existence of tamper-resistant attested cameras. Namely, we assume these cameras produce attested images that are signed with a digital signature. We further assume that the cameras cannot be tampered with (i.e., cannot be made to produce images that were not taken by the camera but signed).

Given the existence of tamper-resistant attested cameras, ZK-IMG *only* assumes the standard ZK-SNARK security model [5] and a collision-resistant hash function [28]. Informally, the ZK-SNARK security assumptions state that the prover (the producer of the image) and verifier (consumers of the media) interact only through the ZK-SNARK and that adversaries (the producer of the image) is computationally bounded.

Under these standard security assumptions, ZK-IMG inherits the zero-knowledge, non-interactive, knowledge-soundness, and completeness properties. In particular, ZK-IMG will produce valid proofs of correctly applied transformations and adversaries will not be able to produce invalid proofs.

While ZK-IMG preserves the zero-knowledge property of the inputs and transformations, and completeness, there are other ways to attack media consumers that are outside of the scope of this work. We describe these below.

Limitations. As described, ZK-IMG only preserves the zero-knowledge property of the input image and intermediate transformations in the ZK-SNARKs. In particular, the revealed output image may leak sensitive information if the transformations did not properly hide the sensitive parts of the image. Such leakage is orthogonal to this work.

Furthermore, ZK-IMG can only attest that the transformations of an attested image were applied properly. Adversaries can manipulate the physical surroundings to produce images that are attested but misleading. These adversaries could also take an image of a deepfake. Validating such imagery is also orthogonal to this work. However, we believe that using attested 3D depth information could help mitigate these issues, such as LIDAR sensor data.

7 Efficiently Proving Single Image Transformations

We first describe how ZK-IMG can produce ZK-SNARK proofs for single image transformations. Although ZK-SNARKs allow arbitrary computations to be proven, we focus on common image transformations that perform “physical” transformations (e.g., crops, rotations) or are the result localized pixel computations (e.g., blurring, colorspace conversions, white balance adjustment).

Transformation	Description
Crop	Extract rectangular sub-image
Rotate	Rotate image
Flip	Flip image across x- or y-axis
Translate	Move image across x- or y-axis
Resize	Change image resolution
Censoring	Selectively black out pixels
RGB to YCbCr	Color space conversion
YCbCr to RGB	Color space conversion
White balance	Adjust white balance
Contrast	Adjust contrast
Sharpen	Apply sharpen filter
Blur	Apply blur filter

Table 1: Summary of image transformations currently implemented in ZK-IMG. These transformations are composable. Furthermore, other transformations can be implemented in ZK-IMG.

One key requirement for ZK-IMG is to allow application developers to add additional transformations. In order to enable extensibility, ZK-IMG uses the ZK-SNARK verification key to specify the computation and the proof to verify that the computation was done correctly. As a result, application developers do not need to develop proving arguments that are specific to transformations and can instead use the primitives ZK-IMG provides.

To preserve the privacy of intermediate results for transformations, ZK-IMG will hash the input and output and reveal the hashes. Under standard cryptographic assumptions of collision-resistant hashes, revealing hashes will reveal nothing about the input data [28]. ZK-IMG will only reveal the final image. As we describe below, this enables optimizations for many transformations. We describe ZK-IMG’s full procedure for chaining transformations in Section 8.

In the remainder of this section, we describe how ZK-IMG uses the Plonkish arithmetization to express common operations and how to implement specific image transformations in ZK-IMG.

7.1 Common Operations

We now describe how to perform copying, division, and dot products in the Plonkish arithmetization. These operations are used across several image transformations as building blocks.

Copying. One common operation is to copy the value from one cell to another. The Plonkish arithmetization allows copying of cells to be done via the permutation argument. This is easily specified in `halo2`. Importantly, the set of copied cells (which are constrained to be equal to each other) can be extracted from the verification key.

Division. Another common operation is integer division with a known, positive divisor. Division is required to do fixed point arithmetic, which approximates floating point arithmetic. As mentioned, the Plonkish arithmetization performs all operations in a large finite field, which does not contain a native division operation.

In order to represent division, we first consider the case of non-negative dividend. Let $b = \lfloor \frac{c}{a} \rfloor$. Then, we have that

$$c = b \cdot a + r$$

where $0 \leq r < a$ is the integral remainder. Since the divisor a is known ahead of time, we can constrain the division with three cells and a lookup constraint. Namely, we lay out three cells with values c , b , and r with the constraint that $c = b \cdot a + r$. We further constrain that r be in the range $0, \dots, a - 1$ and b to be in a valid range (the valid range of b depends on the operation and can be computed ahead of time).

Dot products. The last common operation we describe are dot products. Dot products are used for applying convolutional filters as image transformations and also for pixel-level adjustments.

In particular, given vectors \vec{a} and \vec{b} , we wish to constrain that $c = \vec{a} \cdot \vec{b}$. To do so, we can simply have the constraint that

$$c = a_1 \cdot b_1 + \dots + a_n \cdot b_n$$

and assign c, a_i, b_i to $2n + 1$ cells. If one of the vectors is known ahead of time (e.g., a fixed filter), the values can be omitted and instead hard-coded into the constraint. This reduces the number of assigned cells to $n + 1$ at the cost of adding an additional selector.

Hashes. The `halo2` library contains several hash function implementations, which we use. In this work, we assume that the camera produces the Poseidon hash [14] when the pixels are packed into the field element. As we show, the hashing is by far the dominant cost of our circuits.

7.2 Example Transformations

Given the building blocks we have described, we describe how to use them to construct common image transformations. For brevity, we describe a representative sample of image transformations. The other image transformations in Table 1 can be implemented similarly.

Crop. An image crop takes an image and returns a rectangular subset of the image. Crops can be used to remove sensitive information.

Since a cropped image is a subset of the input image, it can be done entirely through copies. In particular, from an application developer perspective, a crop is equivalent to copying a fixed set of cells. From a verifier perspective, a crop is defined by the set of constraints on the cells.

Image translations, rotations, flips, and nearest neighbor resizing can be done similarly.

Selective removal. A selective removal transformation selectively fills in a fixed set of pixels with black pixels. The fixed set of pixels is typically a rectangle (e.g., a portion of a document) or oval (e.g., a person’s face). The application developer may choose which patterns are permissible. This transformation can be used to censor sensitive parts of the image, such as people’s faces, signs, or documents.

Similar to cropping, the selective removal transformation copies the non-censored pixels from the original image. The censored pixels are copied from a revealed cell that contains the value 0.

Blur. An image blur takes an image and returns an image with a subset of the image with the blur filter applied. Similarly to crops, blurs can be used to remove sensitive information. We describe how to blur the whole image (which is the most resource intensive version), but any subset of the image can be blurred by combining the blurred pixels with copied pixels from the original image.

One common method of applying a blur is to apply a standard Gaussian blur filter, which is a convolutional filter, over the image [30]. A convolutional filter is a local filter in which pixels nearby the target pixel are combined in a fixed way. Namely,

$$y[m, n] = \sum_{i=-c}^c \sum_{j=-c}^c x[m-i][n-j] \cdot h[i][j].$$

for a convolutional filter h of size $(2c+1) \times (2c+1)$.

To implement the Gaussian blur filter, we perform the following operation per pixel. We perform the unrolled convolution as a dot product and divide the result by the fixed point scalar. The result of the division is the clamped to the valid image range (0 to 255).

Other filters, such as a sharpening filter, can be implemented similarly.

Contrast. A contrast adjustment transformation takes an image and increases or decreases the contrast of the image. Adjusting the contrast of the image can highlight details that may be difficult to see in the unadjusted image.

One common way to adjust the contrast is to adjust each sub-pixel value p by some factor $f \in \mathbb{R}^+$ in the following way:

$$p' = \text{RoundAndClip}(128 + f \cdot (p - 128), 0, 255)$$

where `RoundAndClip` rounds the argument to the nearest integer and clips to 0 to 255 (the standard `uint8` range).

To implement the contrast adjustment, we can use a single lookup table. In particular, p takes 256 possible values. Since f is known ahead of time, we can encode the mapping $p \rightarrow p'$ with a lookup table.

Other transformations, such as white balance adjustments (which is also a per-sub-pixel map), can be done similarly. Transformations that require full-pixel computations may require additional computation, such as divisions or other constraints.

Color space conversion (RGB to YCbCr). A color space conversion transforms an image from one color space to another. These conversions are often done before applying an image transformation that is more amenable to the converted colorspace. For example, a luminance adjustment requires only adjusting the Y value in the YCbCr colorspace, but requires complex pixel computations in the RGB colorspace. We describe how to convert RGB to YCbCr.

Given the sub-pixel R, G, and B values in RGB color space, we can compute the Y, Cb, and Cr sub-pixel values in YCbCr as follows [17]:

$$\begin{aligned} Y &= 0 & + (0.299 \cdot R) & + (0.587 \cdot G) & + (0.114 \cdot B) \\ Cb &= 128 & - (0.168736 \cdot R) & - (0.331264 \cdot G) & + (0.5 \cdot B) \\ Cr &= 128 & + (0.5 \cdot R) & - (0.418688 \cdot G) & - (0.081312 \cdot B) \end{aligned}$$

in floating point. We can convert the floating point operations to fixed point by multiplying all values by a scalar and rounding to the nearest integer. The resulting value can be cast back to the valid range using division as described above. The Y, Cb, and Cr values are rounded to the nearest integer. They need not be clamped due to the range of admissible values.

There are several choices of possible implementations for the RGB to YCbCr color space conversion. One method would be to have a lookup table for the full pixel values. However, this requires a lookup table of size 2^{24} , which would force the grid to have at least 2^{25} rows, as several additional rows are required to ensure the zero-knowledge property. Requiring so many rows is resource intensive. Nonetheless, it requires fewer columns (two per pixel).

In many circumstances, it is too resource intensive to have 2^{25} rows. As such, we can implement the RGB to YCbCr color space conversion by explicitly computing the linear functions. Each sub-pixel in YCbCr can be computed as a dot product with known constants and a linear offset (0 or 128). As described above, we can approximate the floating point arithmetic with fixed point arithmetic. Finally, we can divide the results of the fixed point arithmetic by the exponent. Clamping is not necessary as the domain constrains the range to be in 0 to 255.

Other colorspace conversions can be implemented similarly.

Other transformations. As shown in Table 1, we implement several other transformations. These transformations largely follow the pattern of selectively copying pixels and local transformations. Our API allows these patterns to be implemented so they can be easily added and composed.

7.3 Optimizations

As described in Section 4, there are several important considerations in the performance of the `halo2` proving system and Plonkish arithmetization. We describe several optimizations to improve the performance of the arithmetic circuits. Several similar optimizations were explored in the context of executing machine learning models [18].

Circuit size and packing rows. One of the most critical factors to performance is circuit size. Circuit size is determined by the number of rows and columns in the circuit. As we described in Section 4, the number of rows must be a power of two. Importantly, for circuit layout, there are sharp phase transitions in circuit size. Furthermore, the memory pressure substantially increases with each power of two.

Naively laying out our circuits would place one operation per row. However, this can be memory inefficient. Namely, for a fixed number of cells, a circuit with fewer rows and more columns is generally more memory efficient.

As such, ZK-IMG will pack as many operations per row as possible. In particular, since the image transformations are largely local pixel computations, ZK-IMG will lay out per-pixel computations and repeat them as many times as possible per row.

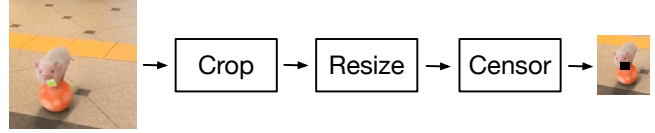
For a fixed number of rows, ZK-IMG will optimize the column count by choosing the minimum number of columns needed for the transformations and hashes. ZK-IMG will similarly optimize the number of rows for a fixed number of columns. There is a fixed minimum number of operations required for the hashes, which constrains the minimum number of rows. ZK-IMG will estimate the total cost of various configurations of rows and columns and pick the minimum cost plan under the memory constraints.

Hard-coding transformation-specific operations. As described above, ZK-IMG provides the verification key in addition to the proof certificate. The verification key encodes the transformations on a per-transformation basis, so application developers need not construct custom arguments for all possible transformation parameters.

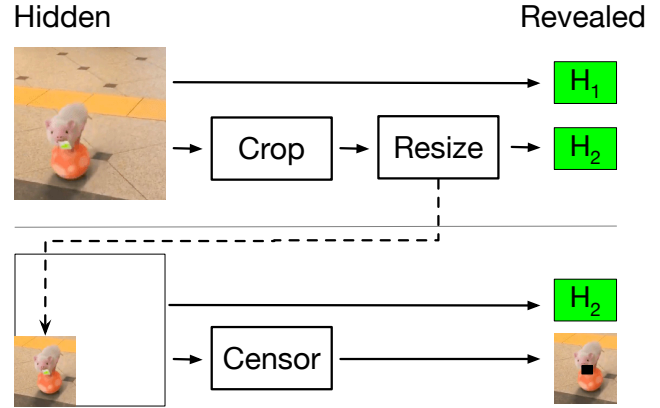
In addition to relieving developer effort, per-transformation circuits allow ZK-IMG to perform optimizations. In particular, wherever possible, ZK-IMG will avoid copying values into new cells and will hard-code as many values as possible into custom gates.

As an example of avoiding copies to new cells, consider the operation of a crop, which extracts a subset of an image. Instead of copying the values into new cells in the crop, ZK-IMG can instead return the subset of cells from the input. These cells can subsequently be transformed, hashed, or revealed. This optimization can make intermediate transformations *free* in terms of prover and verifier cost.

As an example of hard-coding transformation-specific values, consider the blur operation. Instead of laying out the filter values, they can be directly encoded in the custom gate as



(a) Example of a series of image transformations which hides sensitive information (the card in the pig’s mouth).



(b) Example of splitting the image transformations across multiple ZK-SNARKs while preserving intermediate transform privacy. Only the hashes (H_1, H_2) and final image are revealed.

Figure 2: Schematic of ZK-IMG’s procedure to split transformations across ZK-SNARKs while hiding intermediate images.

the constraint. This can save nearly $2\times$ the number of cells, greatly reducing the computational burden.

Sharing lookup tables. A number of operations require lookup tables. For example, they may be used to perform division or clamp a value.

Wherever possible, ZK-IMG will reuse lookup tables. In particular, a common operation is a clamping operation, which performs

$$\text{Clamp}(x) = \text{Max}(\text{Min}(x, 255), 0).$$

Given the range of possible values of x , we can construct two lookup tables for the input and output respectively. These lookup tables can be shared across transformations that require the clamping operator.

Similarly, ZK-IMG can reuse division remainder range checks for operations that use the same scale factor.

8 Securely Chaining Image Transformations

In many circumstances, the initially attested image is edited with several transformations before being released. For example, a typical series of transformations may include a crop and censoring (to hide sensitive information), white balance adjustment, sharpen, and contrast adjustment (for increased

legibility), and a resize (to transform the image to a standard size).

One such way to chain a series of image transformations would be to do all the transformations in a single circuit. Unfortunately, this increases the computational burden of creating the ZK-SNARK proof. In particular, increasing the circuit size increases the memory burden of proving, which can result in insufficient memory resources.

Another way to chain transformations would be to ZK-SNARK individual transforms and release the intermediate images. Unfortunately, revealing the intermediate images compromises the privacy guarantees of the ZK-SNARKs (otherwise, the initial image could have been released).

To address this issue, ZK-IMG will split image transformations across ZK-SNARK proofs. However, instead of releasing the intermediate images, ZK-IMG will exhibit a private witness (i.e., the pixel values in the intermediate image) and hash the intermediate image in the ZK-SNARK. ZK-IMG will only reveal the hashes of the intermediate images, not the pixel values themselves. We show a schematic of this process in Figure 2.

This raises a natural question: how should ZK-IMG pack transformations between ZK-SNARKs given limited memory resources? Every extra ZK-SNARK proof adds an additional hash operation, which is expensive. As such, ZK-IMG aims to reduce the total number of ZK-SNARK proofs. ZK-IMG will do this by cost modeling the transformations and packing as many transformations as possible per ZK-SNARK proof subject to the memory limit.

9 Evaluation

In this Section, we evaluate ZK-IMG on a range of image transformations and settings. We show that ZK-IMG can produce proofs that can be verified in as little as 5.6ms on HD image transformations. We further show that ZK-IMG’s image transformation implementations are efficient, taking as few as 7.5s to prove. When implemented end-to-end (which no other work has done), ZK-IMG can prove transformations on commodity hardware with as little as \$0.48 per image.

9.1 Evaluation Setup

We evaluated ZK-IMG on one or more image transformations, both end-to-end (i.e., secured by hashing the inputs/outputs) and the transformations themselves. For consistent results, we use the Amazon Web Services (AWS) `r6i.16xlarge` instance, which has 64 vCPU cores and 512 GB of memory. While large, widely available desktop devices (e.g., the Mac Pro) has similar amounts of resources. We defer a full discussion of hardware limitations to Section 9.6.

We measured the time to generate the ZK-SNARK proof (i.e., the time for the producer of the image to prove the transformations), the verification time (i.e., the time for the image

consumer to verify the proof), the proof size, and peak memory usage (using `heaptrack`). Where applicable, we further estimate dollar costs of the proving time using AWS spot instances.

To compute the hashes of inputs and outputs, we use the Poseidon hash function [15], which can be implemented efficiently in ZK-SNARKs. We use a width of 3 rate of 2, which gives 128 bits of security. As we show, computing the hashes is by far the dominant cost of end-to-end image transformations.

9.2 Evaluating Transformations

ZK-IMG performance. We first benchmark our implementations of single image transformations. Several of our transformations are implemented logically when combined with other transformations (crops, rotations, censoring, etc.). For these transformations, we benchmarked the versions that copied the values from the input.

Our implementation of the transformations in ZK-IMG can take as little as 7.8 seconds to prove and 5.6 ms to verify (Table 2). Our most expensive transformation (the convolution) takes 82 seconds to prove and 8.1 ms to verify. The maximum peak memory usage across transformations is 15.7 GB.

As these results show, ZK-IMG’s implementations of image transformations are efficient and can transform HD images on widely available laptops (e.g., the MacBook Pro). These results demonstrate the feasibility of verifying high quality images.

Comparison to PhotoProof. The closest work we are aware of is PhotoProof [25]. PhotoProof verifies the signatures and hashes outside of the ZK-SNARKs, which can be done if the intermediate images are revealed. The implementation of PhotoProof was not available at the time of writing and authors did not respond to our correspondences to make their code available.

To compare against PhotoProof, which applies a single image transformation at a time, we executed ZK-IMG on contrast, the most expensive operation PhotoProof considered. We further matched hardware as closely as possible by using the `r6i.xlarge` instance, which had 4 vCPU cores (half as many threads as in the evaluation of [25]) and 32 GB of RAM. We used 128×128 images as in PhotoProof.

PhotoProof requires 306 seconds to prove (ignoring the cost of key generation) and 500ms to verify transformations on 128×128 images. In contrast, ZK-IMG takes 2.74 seconds to prove (including the cost of key generation) and 5.3ms to verify, which corresponds to a $112 \times$ and $94 \times$ speedup, respectively.

Comparison to no privacy alternative. We then asked how ZK-IMG’s performance compared to the no privacy alternative. Namely, the owner of the image releases the attested

Transformation	Key generation	Proving	Verification	Proof size	Peak memory usage
Crop (HD \rightarrow SD)	5.63s	7.8s	6.10ms	7040 bytes	1.72 GB
Resize (HD \rightarrow SD)	5.60s	7.5s	5.84ms	7040 bytes	1.72 GB
Contrast	14.4s	14.3s	5.57ms	5088 bytes	4.08 GB
White balance	16.1s	15.7s	5.76ms	5792 bytes	4.63 GB
RGB2YCbCr	31.5s	65.9s	9.39ms	14592 bytes	11.0 GB
YCbCr2RGB	31.9s	67.7s	10.1ms	14592 bytes	11.0 GB
Convolution	69.8s	81.7s	8.14ms	11200 bytes	15.74G

Table 2: Performance measurements for ZK-IMG’s image transformation implementations. Our implementations are efficient: they can take as few as 5.6 ms to verify, as few as 7.5s to prove, and require a peak memory usage of at most 15.7GB. As shown, our transformations can be done on commodity laptops.

Operation	ZK-IMG	No privacy
Contrast	6.27ms	9.82ms
White Balance	6.22ms	8.34ms
RGB2YCbCr	6.50ms	13.24ms
YCbCr2RGB	5.44ms	13.04ms
Convolution	4.69ms	78.25ms

Table 3: Verification time of ZK-IMG with privacy and a no-privacy alternative for various image transformations. As shown, ZK-IMG outperforms on verifying images.

image publicly and the verify performs the transformations directly.

We implemented the transformations in Rust and benchmarked the time to perform the transformations. As shown in Table 3, the cost of performing the transformations directly can actually be greater than the cost of verifying the transformations. Although surprising, ZK-SNARKs can provide sub-linear verification of computations.

9.3 Evaluating End-to-End Transformations

We then benchmarked ZK-IMG on end-to-end image transformations, when including the hash of the inputs. This can be used to keep the privacy of the input data.

As shown in Table 4, the verification times are still minimal: at most 8.0 ms. Unfortunately, the hashing can be up to $20\times$ slower than the image transformation itself for proving. This can result in proving times up to 617 s and peak memory usage up to 102 GB. Nonetheless, these operations can be run on powerful, commercially available desktops (e.g., the Mac Pro). Furthermore, these transformations can cost as little as \$ 0.28 on cloud hardware.

9.4 Evaluating End-to-End Hidden Images

We then benchmarked ZK-IMG on end-to-end image transformations, when including hashes of the inputs and outputs. This can be used for producing attestations to hidden images.

Namely, for each operation, we measured the performance when hashing the input and output.

As shown in Table 5, the verification times are still minimal: at most 15.4 ms (a sublinear increase compared to a single hash). As with input privacy preserving transformations, hashing the output can dramatically increase the proving overheads of image transformations. This can result in proving times up to 2236s and peak memory usage up to 308 GB. Nonetheless, these operations can be run on powerful, commercially available desktops (e.g., the Mac Pro) as before. Furthermore, these transformations can cost as little as \$0.48 on cloud hardware.

The cost of some operations (crop, resize) are substantially cheaper than the cost of others. This is because for both the crop and resize, the output image is SD (720×480), which contains $2.7\times$ fewer pixels compared to HD images. Since hashing is the predominant cost, this results in substantially cheaper output hashes, which decreases the key generation time, proving time, and peak memory usage.

9.5 Developer Effort

We asked how much developer overhead ZK-IMG requires. To measure this, we compared the number of lines of code that implementing transformations in ZK-IMG required compared to manually implementing the transformations without privacy in Rust. We measured the lines of code for the transformations only in ZK-IMG, transformations with boilerplate code in ZK-IMG, and our no-privacy, expert-coded transformations in Rust. The boilerplate code in ZK-IMG is required to interface with the `halo2` library.

We show results in Table 6. As shown, ZK-IMG’s transformations can be written in as few as 20 lines of code. The developer effort increases with the complexity of the transformation, but remains manageable, under 232 lines of code in all settings.

9.6 Discussion of Results

As we have shown, ZK-IMG is able to transform images efficiently, with peak memory usage of 15.7 GB and verification

Transformation	Key generation	Proving	Verification	Proof size	Peak memory usage
Crop (HD \rightarrow SD)	246.1s	328.2s	6.90ms	3040 bytes	70.7 GB
Resize (HD \rightarrow SD)	246.6s	328.2s	5.33ms	3040 bytes	70.7 GB
Contrast	283.1s	363.8s	6.27ms	3712 bytes	85.3 GB
White balance	293.9s	359.6s	6.22ms	3776 bytes	87.9 GB
RGB2YCbCr	276.3s	617.5s	7.96ms	6496 bytes	89.1 GB
YCbCr2RGB	276.2s	606.9s	8.02ms	6496 bytes	89.1 GB
Convolution	339.5s	428.5s	4.69ms	4672 bytes	102.2 GB

Table 4: Performance measurements of ZK-IMG’s image transformations when including the hash of the input. Despite requiring more computational resources for proving, the proofs can be verified in as little as 4.7 ms and at most 8.0 ms. Unfortunately, the hash can take up to 95% overhead for proving, requiring dramatically more time and memory.

Transformation	Key generation	Proving	Verification	Proof size	Peak memory usage
Crop (HD \rightarrow SD)	432.6s	557.1s	6.22ms	6112 bytes	139.1 GB
Resize (HD \rightarrow SD)	431.8s	556.8s	5.62ms	6112 bytes	139.1 GB
Contrast	823.8s	1029.1s	8.16ms	12608 bytes	284.3 GB
White balance	839.4s	1027.9s	8.60ms	12672 bytes	287.1 GB
RGB2YCbCr	816.1s	2198.0s	15.4ms	26144 bytes	307.9 GB
YCbCr2RGB	815.5s	2236.2s	14.8ms	26144 bytes	307.9 GB
Convolution	897.9s	1300.3s	9.32ms	15232 bytes	305.3 GB

Table 5: Performance measurements of ZK-IMG’s image transformations when including the hash of the input and output. Despite requiring more computational resources for proving, the proofs can be verified in as little as 5.6ms and at most 15.4ms. Unfortunately, the hash can take up to 95% overhead for proving, requiring dramatically more time and memory.

Operation	ZK-IMG	ZK-IMG + boilerplate	No privacy
Crop	20	52	12
Resize	39	74	18
Contrast	112	132	9
White balance	135	157	8
RGB2YCbCr	192	212	24
YCbCr2RGB	212	232	26
Convolution	174	195	23

Table 6: Lines of code to implement ZK-IMG’s transformations and the no-privacy versions. Even the most complex transformation requires at most 232 lines of code.

times as low as 5.9ms. However, when including the hashes of the inputs and outputs, the peak memory usage increases to 305 GB. Although feasible on a powerful desktop, this limits the feasibility of deploying ZK-IMG widely. In particular, there are modern image editing methods which leverage deep neural networks (that no prior work addresses) that are currently computationally expensive, although possible to implement in ZK-IMG.

Fortunately, there are several ways to improve the performance of ZK-IMG; we highlight several such methods. First, proving systems are rapidly improving. Recent advances in proving systems can asymptotically reduce the memory usage from $O(n \log n)$ to $O(n)$ [6] while simultaneously improving

proving times. Second, ZK-SNARK-friendly hash functions are rapidly being developed. Since the hashing operations take up to 95% of the computational resources, any developments in improved ZK-SNARK-friendly hash functions will also dramatically improve ZK-IMG. Third, ZK-SNARKs are amenable to hardware acceleration [22, 38]. We hope that improvements in ZK-SNARK technology will unlock widespread availability of verified images and that ZK-IMG can serve as a platform for such work.

10 Related Work

Attested cameras. Attested cameras digitally sign images immediately on capture to ensure the validity of an image [10]. These cameras can be purchased on the market today, such as Sony’s Alpha 7 IV camera [32]. Although they can sign the images on capture, they cannot attest to image transformations of the initially captured image. In this work, we focus on the problem of attesting to downstream image transformations.

Provable image transformations. Several prior research projects have designed systems for verified image transformations [8, 20, 25]. However, this work has three major drawbacks as we have described: they require *the original image to be revealed* [8, 25], only operates on impractically small images (128×128) [8, 25], or require specific cryptographic arguments for new image transformations [20, 25]. In this

work, we scale zero-knowledge image transformations to HD images, provide a secure method of chaining together arbitrary image transformations arbitrarily many times.

Other cryptographic primitives. There are a range of other cryptographic primitives that can provide privacy or security. Two popular methods are multiparty computation (MPC) and homomorphic encryption (HE). MPC allows multiple parties to compute a function without revealing information about the inputs or intermediate states [11]. Unfortunately, MPC requires that all parties be online during the duration of the computation. As a result, it is not suitable for our setting. HE allows parties to perform computation over encrypted data without first decrypting the data [2]. Unfortunately, HE is incredibly expensive. In our setting, this would place the burden of computation on the consumers of the images, which may be consumer devices such as laptops or phones. As such, it is infeasible to use HE in our setting.

Deepfake detection. Aside from using cryptographic primitives, the literature has proposed detecting deepfakes to combat them [23]. There are a range of benchmarks [9, 41] and techniques proposed to detect deepfakes [7, 16, 40]. While promising, there are a number of challenges with these methods. As with other security problems, deepfakes are rapidly evolving, with generation capabilities improving rapidly. Detection methods that work now may not work in the future. Furthermore, adversarial examples [13] can attack deepfake detection methods. In this work, we propose instead to use ZK-SNARKs to attest that images were taken by a particular camera instead, which bypasses such issues.

11 Conclusion

In this work, we present ZK-IMG, the first system for attesting to arbitrarily transformed images at HD scale. ZK-IMG accomplishes this by producing ZK-SNARK proofs of arbitrary image transforms and chaining sequences of proofs in a secure manner. ZK-IMG is able to attest to HD images on commodity hardware, producing proofs that take as little as 5.6 milliseconds to verify. Furthermore, application developers are able to extend ZK-IMG with new image transformations. We hope that ZK-IMG serves as a platform for research in attested images.

Acknowledgments

This work is supported in part by the Open Philanthropy project.

References

[1] Hunt Allcott, Matthew Gentzkow, and Chuan Yu. Trends in the diffusion of misinformation on social media. *Re-*

search & Politics, 6(2):2053168019848554, 2019.

- [2] Frederik Armknecht, Colin Boyd, Christopher Carr, Kristian Gjøsteen, Angela Jäschke, Christian A Reuter, and Martin Strand. A guide to fully homomorphic encryption. *Cryptology ePrint Archive*, 2015.
- [3] Nir Bitansky, Ran Canetti, Alessandro Chiesa, Shafi Goldwasser, Huijia Lin, Aviad Rubinfeld, and Eran Tromer. The hunting of the snark. *Journal of Cryptology*, 30(4):989–1066, 2017.
- [4] Mark Bowden. The hunt for “geronimo”, 2012. URL: <https://archive.vanityfair.com/article/2012/11/the-hunt-for-geronimo>.
- [5] Benedikt Bünz, Ben Fisch, and Alan Szepieniec. Transparent snarks from dark compilers. In *Annual International Conference on the Theory and Applications of Cryptographic Techniques*, pages 677–706. Springer, 2020.
- [6] Binyi Chen, Benedikt Bünz, Dan Boneh, and Zhenfei Zhang. Hyperplonk: Plonk with linear-time prover and high-degree custom gates. *Cryptology ePrint Archive*, 2022.
- [7] Davide Alessandro Cocomini, Nicola Messina, Claudio Gennaro, and Fabrizio Falchi. Combining efficientnet and vision transformers for video deepfake detection. In *International Conference on Image Analysis and Processing*, pages 219–229. Springer, 2022.
- [8] Trisha Datta and Dan Boneh. Using zk proofs to fight disinformation, 2022. URL: <https://medium.com/@boneh/using-zk-proofs-to-fight-disinformation-17e7d57fe52f>.
- [9] Brian Dolhansky, Joanna Bitton, Ben Pflaum, Jikuo Lu, Russ Howes, Menglin Wang, and Cristian Canton Ferrer. The deepfake detection challenge (dfdc) dataset. *arXiv preprint arXiv:2006.07397*, 2020.
- [10] Gary L Friedman. The trustworthy digital camera: Restoring credibility to the photographic image. *IEEE Transactions on consumer electronics*, 39(4):905–910, 1993.
- [11] Oded Goldreich. Secure multi-party computation. *Manuscript. Preliminary version*, 78:110, 1998.
- [12] Josh Goldstein. How disinformation evolved in 2020, 2021. URL: <https://www.brookings.edu/techstream/how-disinformation-evolved-in-2020/>.
- [13] Ian J Goodfellow, Jonathon Shlens, and Christian Szegedy. Explaining and harnessing adversarial examples. *arXiv preprint arXiv:1412.6572*, 2014.

- [14] Lorenzo Grassi, Dmitry Khovratovich, Christian Reberger, Arnab Roy, and Markus Schofnegger. Poseidon: A new hash function for zero-knowledge proof systems. Cryptology ePrint Archive, Paper 2019/458, 2019. <https://eprint.iacr.org/2019/458>. URL: <https://eprint.iacr.org/2019/458>.
- [15] Lorenzo Grassi, Dmitry Khovratovich, Christian Reberger, Arnab Roy, and Markus Schofnegger. Poseidon: A new hash function for {Zero-Knowledge} proof systems. In *30th USENIX Security Symposium (USENIX Security 21)*, pages 519–535, 2021.
- [16] Luca Guarnera, Oliver Giudice, and Sebastiano Battiato. Deepfake detection by analyzing convolutional traces. In *Proceedings of the IEEE/CVF conference on computer vision and pattern recognition workshops*, pages 666–667, 2020.
- [17] Eric Hamilton. Jpeg file interchange format. 2004.
- [18] Daniel Kang, Tatsunori Hashimoto, Ion Stoica, and Yi Sun. Scaling up trustless dnn inference with zero-knowledge proofs. *arXiv preprint arXiv:2210.08674*, 2022.
- [19] Aniket Kate, Gregory M Zaverucha, and Ian Goldberg. Constant-size commitments to polynomials and their applications. In *International conference on the theory and application of cryptology and information security*, pages 177–194. Springer, 2010.
- [20] Hankyung Ko, Ingeun Lee, Seunghwa Lee, Jihye Kim, and Hyunok Oh. Efficient verifiable image redacting based on zk-snarks. In *Proceedings of the 2021 ACM Asia Conference on Computer and Communications Security*, pages 213–226, 2021.
- [21] Jason Law. Better business bureau warns about “deepfake elon musk” investment scam. 2022. URL: <https://www.boston25news.com/news/local/better-business-bureau-warns-about-deepfake-elon-musk-investment-scam/S35FGICEKJADDC4SUHE7FEFJM4/>.
- [22] Tao Lu, Chengkun Wei, Ruijing Yu, Yi Chen, Li Wang, Chaochao Chen, Zeke Wang, and Wenzhi Chen. cuzk: Accelerating zero-knowledge proof with a faster parallel multi-scalar multiplication algorithm on gpus. *Cryptology ePrint Archive*, 2022.
- [23] Siwei Lyu. Deepfake detection: Current challenges and next steps. In *2020 IEEE international conference on multimedia & expo workshops (ICMEW)*, pages 1–6. IEEE, 2020.
- [24] Modems. 71% of people edit their selfies. 2020. URL: <https://www.themodems.com/beauty/71-percent-of-people-edit-their-selfies>.
- [25] Assa Naveh and Eran Tromer. Photoproof: Cryptographic image authentication for any set of permissible transformations. In *2016 IEEE Symposium on Security and Privacy (SP)*, pages 255–271. IEEE, 2016.
- [26] Dan Patterson. From deepfake to “cheap fake,” it’s getting harder to tell what’s true on your favorite apps and websites. 2019. URL: <https://www.cbsnews.com/news/what-are-deepfakes-how-to-tell-if-video-is-fake/>.
- [27] Aditya Ramesh, Prafulla Dhariwal, Alex Nichol, Casey Chu, and Mark Chen. Hierarchical text-conditional image generation with clip latents. *arXiv preprint arXiv:2204.06125*, 2022.
- [28] Phillip Rogaway and Thomas Shrimpton. Cryptographic hash-function basics: Definitions, implications, and separations for preimage resistance, second-preimage resistance, and collision resistance. In *International workshop on fast software encryption*, pages 371–388. Springer, 2004.
- [29] Robin Rombach, Andreas Blattmann, Dominik Lorenz, Patrick Esser, and Björn Ommer. High-resolution image synthesis with latent diffusion models. In *Proceedings of the IEEE/CVF Conference on Computer Vision and Pattern Recognition*, pages 10684–10695, 2022.
- [30] Linda G Shapiro, George C Stockman, et al. *Computer vision*, volume 3. Prentice Hall New Jersey, 2001.
- [31] Meredith Somers. Deepfakes, explained. 2020. URL: <https://mitsloan.mit.edu/ideas-made-to-matter/deepfakes-explained>.
- [32] Sony. Sony unlocks in-camera forgery-proof technology. 2022. URL: <https://www.sony.eu/presscentre/news/sony-unlocks-in-camera-forgery-proof-technology>.
- [33] Eliza Strickland. Facebook ai launches its deepfake detection challenge. *IEEE Spectrum*, 2019. URL: <https://spectrum.ieee.org/facebook-ai-launches-its-deepfake-detection-challenge>.
- [34] Catherine Stupp. Fraudsters used ai to mimic ceo’s voice in unusual cybercrime case. *Wall Street Journal*, 2019. URL: <https://www.wsj.com/articles/fraudsters-use-ai-to-mimic-ceos-voice-in-unusual-cybercrime-case-11567157402>.
- [35] James Vincent. Binance executive claims scammers made a deepfake of him. 2022. URL: <https://www.theverge.com/2022/8/23/23318053/binance-comms-crypto-chief-deepfake-scam-claim-patrick-hillmann>.

- [36] Jane Wakefield. Deepfake presidents used in russia-ukraine war. *BBC*, 2022. URL: <https://www.bbc.com/news/technology-60780142>.
- [37] Yuxi Wang, Martin McKee, Aleksandra Torbica, and David Stuckler. Systematic literature review on the spread of health-related misinformation on social media. *Social science & medicine*, 240:112552, 2019.
- [38] Charles F Xavier. Pipemsm: Hardware acceleration for multi-scalar multiplication. *Cryptology ePrint Archive*, 2022.
- [39] zcash. halo2, 2022. URL: <https://zcash.github.io/halo2/>.
- [40] Hanqing Zhao, Wenbo Zhou, Dongdong Chen, Tianyi Wei, Weiming Zhang, and Nenghai Yu. Multi-attentional deepfake detection. In *Proceedings of the IEEE/CVF conference on computer vision and pattern recognition*, pages 2185–2194, 2021.
- [41] Bojia Zi, Minghao Chang, Jingjing Chen, Xingjun Ma, and Yu-Gang Jiang. Wilddeepfake: A challenging real-world dataset for deepfake detection. In *Proceedings of the 28th ACM international conference on multimedia*, pages 2382–2390, 2020.